Distribution of particles, small molecules and polymeric formulation excipients in the suprachoroidal space after microneedle injection

Bryce Chiang, *Georgia Institute of Technology*
Nitin Venugopal, *Georgia Institute of Technology*
Henry Edelhauser, *Emory University*
Mark R. Prausnitz, *Emory University*

Journal Title: Experimental Eye Research
Volume: Volume 153
Publisher: Elsevier | 2016-12-01, Pages 101-109
Type of Work: Article | Post-print: After Peer Review
Publisher DOI: 10.1016/j.exer.2016.10.011
Permanent URL: https://pid.emory.edu/ark:/25593/s6qn0

Final published version: http://dx.doi.org/10.1016/j.exer.2016.10.011

HHS Public Access

Author manuscript

Exp Eye Res. Author manuscript; available in PMC 2017 December 01.

Published in final edited form as:

Exp Eye Res. 2016 December ; 153: 101–109. doi:10.1016/j.exer.2016.10.011.

Distribution of Particles, Small Molecules and Polymeric Formulation Excipients in the Suprachoroidal Space after Microneedle Injection

Bryce Chiang[1], **Nitin Venugopal**[2], **Henry F. Edelhauser**[3,*], and **Mark R. Prausnitz**[1,4,†]

[1]Wallace H. Coulter Department of Biomedical Engineering, Georgia Institute of Technology, Atlanta, GA

[2]H. Milton Stewart School of Industrial & Systems Engineering, Georgia Institute of Technology, Atlanta, GA

[3]Emory Eye Center, Emory University, Atlanta, GA

[4]School of Chemical & Biomolecular Engineering, Georgia Institute of Technology, Atlanta, GA

Abstract

The purpose of this work was to determine the effect of injection volume, formulation composition, and time on circumferential spread of particles, small molecules and polymeric formulation excipients in the suprachoroidal space (SCS) after microneedle injection into New Zealand White rabbit eyes ex vivo and in vivo. Microneedle injections of 25–150 μL Hank's Balanced Salt Solution (HBSS) containing 0.2 μm red-fluorescent particles and a model small molecule (fluorescein) were performed in rabbit eyes ex vivo, and visualized via flat mount. Particles with diameters of 0.02 – 2 μm were co-injected into SCS in vivo with fluorescein or a polymeric formulation excipient: fluorescein isothiocyanate (FITC)-labeled Discovisc or FITC-labeled carboxymethyl cellulose (CMC). Fluorescent fundus images were acquired over time to determine area of particle, fluorescein and polymeric formulation excipient spread, as well as their co-localization. We found that fluorescein covered a significantly larger area than co-injected particles when suspended in HBSS, and that this difference was present from 3 min post-injection onwards. We further showed that there was no difference in initial area covered by FITC-Discovisc and particles; the transport time (i.e., the time until the FITC-Discovisc and particle area began dissociating) was 2 d. There was also no difference in initial area covered by FITC-CMC and particles; the transport time in FITC-CMC was 4 d. We also found that particle size (20 nm – 2 μm) had no effect on spreading area when delivered in HBSS or Discovisc. We conclude that (i) the area of particle spread in SCS during injection generally increased with increasing injection volume, was unaffected by particle size and was significantly less than the area of fluorescein spread, (ii) particles suspended in low-viscosity HBSS formulation were entrapped in the SCS

†To whom correspondence should be addressed: prausnitz@gatech.edu.
*Deceased

after injection, whereas fluorescein was not and (iii) particles co-injected with viscous polymeric formulation excipients co-localized near the site of injection in the SCS, continued to co-localize while spreading over larger areas for 2 – 4 days, and then no longer co-localized as the polymeric formulation excipients were cleared within 1 – 3 weeks and the particles remained largely in place. These data suggest that particles encounter greater barriers to flow in SCS compared to molecules and that co-localization of particles and polymeric formulation excipients allow spreading over larger areas of the SCS until the particles and excipients dissociate.

Key Terms

Suprachoroidal space; Microneedle injection; Targeted ocular drug delivery; Tissue distribution in eye

1 Introduction

Ophthalmic drug delivery into the potential space between the sclera and the choroid (aka. suprachoroidal space or SCS), is a new drug delivery technique actively under pre-clinical and clinical investigation (Chen et al., 2015; Einmahl et al., 2002; Gilger et al., 2013; Goldstein, 2015; Ianchulev, 2014; Olsen et al., 2006; Patel et al., 2012; Patel et al., 2011). Unlike traditional ophthalmic drug delivery techniques, such as topical eye drops and intravitreal injections, SCS injection enables targeted delivery to the choroid, retinal pigment epithelium, and retina with high bioavailability (Abarca et al., 2013; Chen et al., 2015; Einmahl et al., 2002; Kadam et al., 2013; Olsen et al., 2011; Patel et al., 2012; Patel et al., 2011; Peden et al., 2011; Tzameret et al., 2014). Additional advantages of SCS delivery include increased bioavailability, dose sparing, and avoiding the visual axis. A hollow-bore needle with a length of ~1 mm or less (aka. microneedle) can be used to reliably access the SCS without piercing the chorioretina (Patel et al., 2012; Patel et al., 2011). Performing such an injection is similar to an intravitreal injection and has been performed in the outpatient clinic setting (Jiang et al., 2007; Patel et al., 2012; Patel et al., 2011). Ongoing clinical trials are assessing the safety and efficacy of microneedle injections for indications such as posterior noninfectious uveitis (NCT01789320 and NCT02595398) (Goldstein, 2015).

When administering drugs via the SCS, it is important to control the area over which the drug formulations spread within the SCS. This targeting within the SCS may be used to treat diseased tissue while sparing non-diseased tissue. In some cases, it is desirable to have drug distributed over a large area of the SCS to broadly deliver drug to the chorioretina (e.g., to treat posterior uveitis (Goldstein, 2015)). In other cases, it may be desirable to localize the drug near the site of injection (e.g., to treat glaucoma)(Chiang et al., 2016a; Kim et al., 2014b).

Previous studies have used the two-dimensional (2D) circumferential spread of particles injected into the SCS as the primary metric of distribution (Kim et al., 2014a, b; Kim et al., 2015; Patel et al., 2012; Patel et al., 2011). Though many studies have investigated the distribution of particles (Chen et al., 2015; Kim et al., 2014a; Kim et al., 2015; Patel et al., 2012; Patel et al., 2011) and molecules (Kim et al., 2014b; Olsen et al., 2011; Patel et al., 2012; Tyagi et al., 2013; Wang et al., 2012) independently, to our knowledge, no study has

examined the distribution of particles and molecules injected into the SCS simultaneously, or imaged the distribution of polymeric formulation excipients in the SCS. Better understanding of how particles move relative to the formulation will enable the rational design of formulations that control particle spreading in the SCS.

The purpose of this work was to investigate particle, molecule and polymeric formulation excipient distribution following microneedle injection into the rabbit SCS. We used formulations previously identified to have different effects on particle spread (Kim et al., 2015) to better understand how particle movement is influenced by formulation. We hypothesize that (i) particles encounter greater barriers to flow in SCS compared to molecules and (ii) co-localization of particles and polymeric formulation excipients allow spreading over larger areas of the SCS until the particles and excipients dissociate.

2 Materials and Methods

All reagents and chemicals were purchased from Sigma-Aldrich (St. Louis, MO) unless otherwise specified. Red-fluorescent polystyrene particles (Excitation: 580 nm; Emission: 605 nm) and green-fluorescent polystyrene particles (Excitation: 505 nm; Emission: 515 nm) with diameters ranging from 0.02 – 2 μm were purchased from Life Technologies (Fluosphere, Carlsbad, CA). Eyes of pigmented Silver Fox and American Blue rabbits (Broad River Pastures, Elberton, GA) and albino New Zealand White rabbits (Pel Freeze, Rogers, AR) were obtained within 1 day after euthanasia and stored in a −80°C freezer until use. All *in vivo* experiments were carried out in albino New Zealand White rabbits (Charles River Laboratories, Wilmington, MA) and were approved by the Georgia Institute of Technology Institutional Animal Care and Use Committee. Practices complied with the ARVO Statement for the Use of Animals in Ophthalmic and Vision Research. Four replicates per experimental group were performed unless otherwise specified.

2.1 *Ex vivo* injection procedure

Extraocular tissues were carefully removed from the rabbit ocular globe. To simulate a physiological intraocular pressure (IOP) of 10–12 mmHg, a water column was raised to ~14 cm and connected to the eye via a 25-gauge needle penetrated through the optic nerve(Kim et al., 2014a). A microneedle (750 μm in length, 33-gauge; kindly provided by Clearside Biomedical, Alpharetta, GA) attached to a 250 μL glass chromatography syringe (National Scientific, Rockwood, TN) was used to make injections. Injections were performed 3 mm posterior to the limbus at the 12 o'clock position (superior) to be as far as possible from anatomical barriers created by the long posterior ciliary artery that impede circumferential flow(Chiang et al., 2016b).

Depending on the experimental condition, each injection consisted of 25 to 150 μL of 0.5% (w/v) red-fluorescent particles (0.2 μm diameter; Excitation: 580 nm; Emission: 605 nm) and 0.025% (w/v) fluorescein suspended in Hank's Balanced Salt Solution (HBSS; Gibco, Life Technologies). After each injection, the needle was held in place for 1 min to minimize reflux(Rodrigues et al., 2011). The eye was then frozen via submersion in 100% ethanol chilled over dry ice 3 min post-injection depending on experimental condition.

2.2 Flat mount to characterize 2D circumferential spread

After SCS injection and freezing, eyes were prepared to assess the 2D spread of particles and fluorescein, as described previously(Chiang et al., 2016b; Kim et al., 2015; Patel et al., 2012). The frozen eye was sliced open from the limbus to the posterior pole to generate eight approximately equidistant scleral flaps. The resulting scleral flaps were splayed open and the frozen vitreous humor, lens, and aqueous humor were removed.

A digital SLR camera (Canon 60D, Canon, Melville, NY) with a 100 mm lens (Canon) was used to acquire brightfield and fluorescence images. Camera parameters were held constant at shutter speed = 1/15 s and aperture = F/2.8. To acquire the area of fluorescein spread, a green optical band-pass filter (520 ± 10 nm; Edmunds Optics, Barrington, NJ) was placed on the lens, and the sample was illuminated by a lamp with the violet setting of a multicolor LED bulb (S Series RGB MR16/E26. HitLights, Baton Rouge, LA). To visualize the location of the red-fluorescent particles, a red filter (610 ± 10 nm; Edmunds Optics) was placed on the lens, and the sample was illuminated with the same lamp switched to green light. The area of green and red fluorescence that was above threshold was calculated for each eye using ImageJ (National Institutes of Health, Bethesda, MD). Thresholding was set manually based on visual inspection of background signal.

2.3 Fluorescent tagging of excipient formulation

To visualize spread of polymer formulation excipients, we fluorescently labeled polysaccharides that have been shown to significantly influence spread of particles within the SCS (Kim et al., 2015) using previously described methods(Nielsen et al., 2010). Carboxymethyl cellulose (CMC; 700 kDa high viscosity, Sigma-Aldrich) has been shown to impede spread of particles, allowing for localized delivery of particles that stay near the injection site (Kim et al., 2014b; Kim et al., 2015). On the other hand, Discovisc (1.65 MDa hyaluronic acid; Alcon Laboratories, Fort Worth, TX) and hyaluronic acid have been shown to promote spread up to 100% of SCS area by a slow process after injection (Kim et al., 2015).

To label CMC, 250 mg of CMC and 10 mg of fluorescein isothiocyanate (FITC) were added to 25 mL of 0.1 M NaOH in DI water. The solution was mixed in the dark at room temperature (22 °C) for 4.5 days. The solution was then transferred into a dialysis tube (30 kDa cutoff, Spectra/Por, Spectrum Laboratories, Rancho Dominguez, CA) in a DI water bath. The water bath was changed daily for 5 days to remove unreacted FITC. The contents of the dialysis tube were transferred into a 50 mL centrifuge tube and frozen prior to vacuum drying. Care was taken to minimize light exposure at all steps to minimize photobleaching. A similar procedure was performed with Discovisc (1.65 MDa hyaluronic acid); 500 μL of Discovisc and 1 mg of FITC were added to 2.5 mL of 0.1 NaOH. The other methods were the same as those used for FITC labeling of CMC.

2.4 *In vivo* SCS injections and image acquisition

Albino rabbits were anesthetized with isoflurane and treated with proparacaine eye drops (Bausch & Lomb, Rochester, NY). All injections were 50 μL in volume and performed 3

mm posterior to the limbus at the supranasal quadrant (4 mm nasal to the edge of the superior rectus extraocular muscle).

To determine the effect of polymeric formulation on particle spread, the following injections (N=4 eyes per group) were performed: [i] 50 μL of 2% (w/v) red-fluorescent particles (0.2 μm diameter) and 0.025% fluorescein (332 Da) in HBSS; [ii] 50 μL of 2% (w/v) red-fluorescent particles (0.2 μm diameter) and 5% FITC-CMC (~700 kDa) in HBSS; [iii] 50 μL of 2% (w/v) red-fluorescent particles (0.2 μm diameter) and 1x FITC-Discovisc (HA ~1.65 MDa and chondroitin sulfate ~22.5 kDa) re-constituted in HBSS.

To determine if particles ranging from 0.02 μm to 2 μm co-localize, the following injections (N=4 eyes per group) were performed: [i] 50 μL of 1% (w/v) red-fluorescent particles (0.2 μm diameter) and 1% (w/v) green-fluorescent particles (0.02 μm in diameter) suspended in HBSS; [ii] 50 μL of 1% (w/v) red-fluorescent particles (0.2 μm diameter) and 1% (w/v) green-fluorescent particles (0.2 μm diameter) suspended in HBSS; [iii] 50 μL of 1% (w/v) red-fluorescent particles (0.2 μm diameter) and 1% (w/v) green-fluorescent particles (2 μm diameter) suspended in HBSS; and [iv] 50 μL of 1% (w/v) red-fluorescent particles (0.02 μm diameter) and 1% (w/v) red-fluorescent particles (2 μm diameter) suspended in unlabeled Discovisc.

At predetermined time points, the animals were imaged with a modified RetCam II system (Clarity Medical Systems, Pleasanton, CA). Prior to imaging, tropicamide (Akorn Pharmaceuticals, Lake Forest, IL), phenylephrine (Akorn Pharmaceuticals), and proparacaine (Akorn Pharmaceuticals) eye drops were given. The built-in fluorescein attachment was used to capture green fluorescence. For the red fluorescence, green light was generated by placing a 575±50 nm bandpass filter (Edmunds Optics) in line with the fiber optic line. A red-emission filter (610 ± 10 nm, Omega Optical, Brattleboro, VT) was placed over the camera to capture red fluorescence. Animals were euthanized with an injection of pentobarbital through the ear vein at the end of the experiment.

Post-processing of the RetCam images was used to generate a collage for each imaging condition, since the camera did not have built-in image stitching algorithms. Co-localization was determined using a previously described method(McDonald and Dunn, 2013). Briefly, the 2D correlation coefficient of the red- and green-fluorescent images was calculated, and compared against the 2D correlation of 100 randomly assigned image pairs using a one-sided unpaired t-test. A low p-value ($\alpha<0.05$) indicated statistically significant co-localization greater than chance, and a high p-value ($\alpha>0.05$) indicated no significant co-localization.

2.5 Statistical analysis

Image analysis was performed using Matlab and ImageJ. Statistical analysis was performed using Prism (Graphpad, La Jolla, CA). Values are presented as the mean ± standard error of the mean (SEM), unless otherwise specified. Two-way ANOVA and Student's t-test analyses ($\alpha = 0.05$) were performed to determine statistical significance.

3 Results

3.1 Distribution of particles and molecules immediately after injection into the SCS

The first objective was to test the hypothesis that the circumferential area of particle coverage increases with increasing injection volume, and that small molecules (fluorescein) spread more than particles. We therefore calculated the percentage area of the SCS that had red and green fluorescence greater than threshold after injection of increasing volumes into the rabbit SCS *ex vivo* using flat mounts (Figure 1).

Consistent with the hypothesis, area covered by fluorescein and particles generally increased with increasing injection volume, although the rate of increase was larger at lower volumes (Figure 1). A linear fit to the data yielded a poor correlation (r^2 = 0.51 for particles and 0.67 for fluorescein), whereas an exponential fit was better (r^2 = 0.90 for particles and r^2 = 0.69 for fluorescein), which is consistent with the observation that area initially increases and appears to approach a plateau value slightly below 50% area coverage for particles and slightly above 50% for fluorescein. We hypothesize that this apparent plateauing behavior is due to anatomical barriers that inhibit coverage in the inferior hemisphere, especially for particles (Chiang et al., 2016b).

For all injection volumes, the fluorescein occupied a larger area than the red-fluorescent particles ($p<0.0001$, ANOVA). The ratio of area covered by fluorescein versus particles was 2.05±0.24 (mean±SEM), which did not significantly depend on injection volume ($p=0.36$, F test). This difference in area could be explained by the higher diffusivity of fluorescein versus particles (which are assumed to transport only by convection). However, diffusion of fluorescein for 3 min after injection is expected to account for an area increase of only ~20% (based on a calculation assuming a fluorescein diffusivity of 4.3×10^{-6} cm^2/s (Culbertson, 2002) and a covered SCS area of ~200 mm^2 in the rabbit eye(Bozkir et al., 1997)). Because this small predicted increase is much less than the roughly two-fold measured increase, this result suggests that there are additional factors at play in the SCS that limit movement of particles relative to small molecules (i.e., fluorescein).

3.2 Distribution of particles and molecules over time after injection into the SCS *in vivo*

We further investigated the role of formulation and time on particle distribution in the SCS. The distribution of red-fluorescent particles suspended with green fluorescently-tagged formulation excipients in HBSS after injection into the SCS of live rabbits was imaged using red and green fluorescence simultaneously. Fluorescence was imaged used RetCam imaging, which was preferred to other non-contact fundus imaging methods, since it enabled visualization of the posterior pole as well as the far periphery (i.e., the injection site). We then calculated the percentage of the SCS area in the composite images that had red/green fluorescence values at least 0.1% of the starting concentration, which we used as a proxy of true coverage; and determined the incidence of co-localization of the red and green fluorescence greater than chance.

To study the distribution of red-fluorescent particles and green-fluorescent fluorescein molecules injected in HBSS (Figure 2), we measured the SCS area over which the particles and fluorescein spread for 21 days after injection in vivo. The particle area coverage was

constant at all time points from 3 min to 14 d post-injection (p=0.99, Sidak's multiple comparison test), with a small decrease in area at 21 d. In contrast, the fluorescein area increased from 3 min to 1 h post-injection before being cleared by 2 d. At the 3 min and 1 h time points, fluorescein covered a larger area than the red particles (p<0.01, Sidak's multiple comparison test). At later time points (14 and 21 d), there was a decrease in thresholded area, which may be due to photobleaching (Kim et al., 2015). Moreover, the time point at which the maximum fluorescein coverage was measured was later than the red particle maximum. Statistical analysis showed that the particles co-localized with fluorescein immediately after injection, but not at later time points. Taken together with the *ex vivo* data, we conclude that particles suspended in HBSS became immobilized immediately post-injection even though fluorescein was able to move within the SCS well after the injection, and was ultimately cleared within 2 days.

We next investigated how the addition of viscous polymeric formulation excipients affected particle distribution over time. When the formulation consisted of red particles suspended in 5% FITC-CMC in HBSS (Figure 3), particle area coverage increased from 3 min until 2 d post-injection (p<0.01, Sidak's multiple comparison test). Then, from 2 d to 35 d, there was no significant change in particle distribution in the SCS (p=0.61, Sidak's multiple comparison test). The co-injected FITC-labeled CMC initially followed a pattern similar to the particles, increasing in area for the first two days (p<0.005, Sidak's multiple comparison test). However, from 2 d until 21 d, the area of FITC-CMC decreased (p<0.005, Sidak's multiple comparison), and from 21 d until 35 d, there was essentially no detectable FITC-CMC in the SCS. The FITC-CMC never occupied an area larger than the red particles (p>0.07, Sidak's multiple comparison test). The maximum red particle coverage and maximum FITC-CMC coverage occurred at the same time point, i.e., 2 d post injection. The last time point of co-localization was at 4 d. This suggests that the particles and FITC-CMC were transported together during the injection and for up to 2 days thereafter, after which the particles remained immobilized and the FITC-CMC was cleared.

When the formulation consisted of red particles suspended in FITC-Discovisc (Figure 4), particle coverage was constant from 3 min to 1 h (p=0.98, Sidak's multiple comparison test), and then increased by 2 d (p<0.05, Sidak's multiple comparison test). There was no significant change in particle coverage from 2 d to 21 d (p>0.24, Sidak's multiple comparison test). The co-injected FITC-labeled Discovisc molecules initially followed a pattern similar to the particles, increasing in area for the first two days (p<0.005, Sidak's multiple comparison test). However, from 2 d until 7 d, the area of FITC-Discovisc decreased (p<0.005, Sidak's multiple comparison), and from 7 d until 21 d, there was essentially no detectable FITC-Discovisc in the SCS. The FITC-Discovisc never occupied an area larger than the red particles (p>0.05, Sidak's multiple comparison test). The maximum red particle coverage and maximum FITC-Discovisc coverage occurred at the same time point, i.e., 2 d post injection. The last time point of co-localization was at 2 d. This suggests behavior similar to that seen with FITC-CMC, where the particles and FITC-Discovisc were transported together during the injection and for up to 2 days thereafter, after which the particles remained immobilized and the FITC-Discovisc was cleared, although the FITC-Discovisc was cleared faster than the FITC-CMC and, on an absolute scale, the area

coverage of FITC-Discovisc and co-injected particles was roughly twice as large as the area coverage of FITC-CMC and co-injected particles.

Considering all of these data (Figure 2 – Figure 4), the spread of particles immediately after injection depended on formulation composition, such that spreading went from smallest to largest with: FITC-CMC (8.5%) < FITC-Discovisc (26%) < HBSS (30%). At 14 d, the rank list for particle coverage for the tested excipients was FITC-CMC (20%) < HBSS (27%) < FITC-Discovisc (46%). The maximum area coverage was achieved at 3 min when formulated only in HBSS, and at 2 d for FITC-CMC and FITC-Discovisc. The particles injected with a low-viscosity formulation (i.e. HBSS only) did not experience a change in area coverage over time. On the other hand, particles injected with viscous polymeric formulations (FITC-CMC and FITC-Discovisc) experienced an increase in coverage of two-fold when comparing coverages at 3 min and 14 d post-injection. Thus, we can conclude that the viscous polymeric formulations prolonged particle transport time compared with the low-viscosity formulation. There was a strong association between transport time compared with viscosity (see Supplementary Information, Figure S1). Initial viscosity of the formulation was a poor predictor of final spread of particles, possibly due to physical crosslinking of CMC (Benchabane and Bekkour, 2008) that effectively increased viscosity after injection and thereby limited spreading (Figure S2).

Fluorescein in HBSS occupied 66% of the visible SCS, which was the largest area of all the fluorescent species injected. In comparison, peak FITC-CMC spreading was 20% of SCS area, and occurred at 2 d. Peak FITC-Discovisc coverage was 63% and occurred at 2 d. Total clearance of the fluorescently-tagged formulation excipients occurred by 2 d for HBSS, 21 d for FITC-CMC, and 14 d for FITC-Discovisc.

Co-localization of particles and the formulation excipients was seen at 3 min for HBSS, from 3 min up until 4 d for FITC-CMC, and 3 min for FITC-Discovisc.

3.3 Effect of particle size on particle distribution over time after injection into the SCS *in vivo*

To determine the effect of particle size on distribution, particles of different sizes (20 nm – 2 μm) were suspended in HBSS and Discovisc and co-injected into the rabbit SCS *in vivo*. Injections used pairwise combinations of red- and green-fluorescent particles of different sizes to determine whether the particles co-localized in the SCS. In all cases, the pairs of co-injected particles all co-localized for at least 4 d post-injection (Figure 5). With all HBSS conditions, particle area did not change with time ($p>0.06$, 2-way ANOVA). For particles in Discovisc, the particle area increased until 2 d for both the 20 nm and 2 μm particles.

4 Discussion

Traditional ophthalmic drug delivery techniques, namely topical eye drops and intravitreal injections, do not precisely target diseased tissues in the posterior segment. Compared with these conventional routes of administration, SCS delivery enables targeted drug delivery to the choroid, retina, ciliary body, and sclera with higher bioavailability (Chiang et al., 2016a; Kim et al., 2014b; Olsen et al., 2011; Patel et al., 2012; Patel et al., 2011; Wang et al., 2012),

and can be performed in the outpatient clinic setting (Goldstein, 2015; Patel et al., 2012; Patel et al., 2011). The extent and distribution of posterior-segment diseases are typically not uniform. For example, glaucoma treatment requires localization near the ciliary body, which is near the site of microneedle injection (Chiang et al., 2016a; Kim et al., 2014b); while noninfectious posterior uveitis requires spreading throughout the SCS (Goldstein, 2015). Deposition within the SCS can be geographically controlled so as to target diseased tissues while sparing non-diseased tissues (Chiang et al., 2016b; Einmahl et al., 2002; Kim et al., 2014a; Kim et al., 2015; Tyagi et al., 2013). In particular, the area of particle spread can be controlled with different excipient formulations (Kim et al., 2015).

4.1 Distribution of particles and small molecules injected into the SCS

One goal of this work was to study the differences in distribution of particles versus small molecules when co-injected into the SCS of rabbits. We found that, with HBSS as the formulation, the area covered by fluorescein was larger than the area covered by particles for all injection volumes tested immediately after injection. On average, the fluorescein occupied an area twice as large as that occupied by particles *ex vivo* and *in vivo*. The difference in area covered could be due either to barriers in the SCS that preferentially limit movement of particles or to increased diffusion of fluorescein in the SCS post-injection relative to the particles. Because the contribution of fluorescein diffusion was estimated to increased coverage by only ~20%, entrapment of particles is the more likely explanation.

Because molecules distributed to cover a larger area than particles in the SCS, the delivery of molecules may be preferred if the goal is to achieve full coverage of the SCS. However, the use of particles (e.g., containing drug molecules for slow release over time (Chiang et al., 2016a; Goldstein, 2015)) may be preferable to injecting free drug molecules, which are usually cleared from the SCS within a day (Gu et al., 2015; Kim et al., 2014b; Olsen et al., 2011; Patel et al., 2012).

4.2 Effect of formulation on distribution of particles

For the purposes of our kinetic studies on the effects of polymeric formulation excipients *in vivo*, we defined transport time as the greater of (a) the time at which particle area stopped changing and (b) the time at which co-localization of particles and formulation excipients stopped. These two criteria demonstrated when the particle and formulation dissociated. The data showed that there was a strong association between transport time and viscosity of the liquid formulation, where increased viscosity facilitated longer transport time (i.e., for days after the injection). In contrast, viscosity of the formulation had a much weaker association with area coverage, probably because certain viscous formulations like CMC may become physically cross-linked, effectively increasing viscosity after injection and thereby limiting spread.

4.3 Effect of particle size on distribution of particles

Particles with diameters ranging from 2 nm to 2 μm co-localized within the SCS independent of particle size. Furthermore, the size of the particles did not influence transport time. Particles of different sizes may be preferred for different applications, such as micron-scale particles to serve as slow-releasing drug delivery systems, nanoscale virus particles as

gene delivery vectors, and micron-sized cells as cell-based therapies. As shown by Kim et al. (Kim et al., 2015), we also showed that that particles spanning two orders of magnitude in size distributed on the SCS to a similar extent with similar kinetics, which should simplify design of particle delivery to the SCS. Of course, other particle parameters may also play a role, such as particle density, shape, surface properties and composition.

4.4 Study limitations

Limitations of the study include use of rabbit eyes, and shortcomings of equipment and measurement methods. There are physiological and anatomical differences between rabbit and human eyes. These species differences may or may not alter SCS distribution. For example, as we showed previously (Chiang et al., 2016b), there are different anatomical barriers in rabbits versus humans that affect circumferential particle spread. Human clinical trials will be needed to investigate SCS distribution, as it applies to human health. This study used *ex vivo* eyes for some studies, which may not be fully representative of living animals. However, the use of *ex vivo* eyes made certain measurements possible; for example, using *ex vivo* (and enucleated) eyes allowed rapid freezing of the eye to stop particle and molecule movement. The distribution of molecules and particles suspended in HBSS was studied in both *ex vivo* and *in vivo* rabbit eyes, and the results were similar, at least initially post-injection.

The RetCam II fluorescent fundus imaging system did not have the ability to automatically stitch image fields together. Instead, collages were used, and this may have introduced errors in the actual coverage of fluorescence (e.g., two neighboring images in the collage may overlap). However, the RetCam allowed visualization into the far periphery (estimated at 220° of the fundus).

4.5 Conclusion

It was previously shown that particles spread over a somewhat larger area in the SCS after injecting 150 and 100 μl compared to 50 μl of HBSS (Gu et al., 2015; Kim et al., 2015). Here, we show that area covered by a small molecule (fluorescein) and particles (0.2 μm diameter) generally increased with increasing injection volume from 25 μl to 150 μl, although the rate of increase was larger at lower volumes. We also found that the ratio of area covered by fluorescein was approximately double that of particles, which did not significantly depend on injection volume. This indicates that fluorescein flows more readily in the SCS, whereas particles encounter more barriers that limit their spreading in the SCS during injection in HBSS.

It was previously shown that molecules injected in HBSS were cleared from the SCS within hours-days (Gu et al., 2015; Olsen et al., 2011; Wang et al., 2012), whereas particles appear not to be cleared at all (Chen et al., 2015; Chiang et al., 2016a; Kim et al., 2015; Patel et al., 2012; Patel et al., 2011). Here, we show that at 3 min and 1 h, fluorescein spread more than particles and that particles co-localized in the SCS with fluorescein only at 3 min. However at later times (i.e., ≥ 2 days), fluorescein was cleared from the SCS. This suggests that particles injected in HBSS became immobilized immediately post-injection even though fluorescein was able to move within the SCS well after the injection.

It was previously shown that particles injected in CMC or Discovisc formulations spread very little immediately after injection, but increased spreading for two days after injection (Kim et al., 2015). Here, we further showed that particles and FITC-CMC or FITC-Discovisc were transported together during the injection (i.e., co-localized to the same areas) and continued to be co-localized for up to two days (FITC-CMC) or four days (FITC-Discovisc). At later times, the particles remained immobilized and the formulation polymers were cleared within one week (FITC-Discovisc) or three weeks (FITC-CMC).

Taken together, these studies will aid in the development of formulations that can be injected via microneedle to control particle spread within the SCS.

Supplementary Material

Refer to Web version on PubMed Central for supplementary material.

Acknowledgments

We thank Cathy Payne (Broad River Pastures) for graciously providing rabbit eye specimens, Machelle Pardue for use of the RetCam, and Donna Bondy for administrative support. This work was carried out at the Institute for Bioengineering and Bioscience and Center for Drug Design, Development and Delivery at Georgia Tech. This work was supported by National Eye Institute grants EY017045 (BC, HFE, MRP), EY022097 (BC, MRP), EY007092 (BC), and EY025154 (BC). HF Edelhauser held, and B Chiang and MR Prausnitz hold microneedle patents and/or patent applications, and HF Edelhauser had and MR Prausnitz has significant financial interest in Clearside Biomedical, a company developing microneedle-based products for ocular delivery. This potential conflict of interest has been disclosed and is overseen by Georgia Institute of Technology and Emory University.

References

Abarca EM, Salmon JH, Gilger BC. Effect of choroidal perfusion on ocular tissue distribution after intravitreal or suprachoroidal injection in an arterially perfused ex vivo pig eye model. J Ocul Pharmacol Ther. 2013; 29:715–722. [PubMed: 23822159]

Benchabane A, Bekkour K. Rheological properties of carboxymethyl cellulose (CMC) solutions. Colloid and Polymer Science. 2008; 286:1173–1180.

Bozkir G, Bozkir M, Dogan H, Aycan K, Guler B. Measurements of axial length and radius of corneal curvature in the rabbit eye. Acta Med Okayama. 1997; 51:9–11. [PubMed: 9057929]

Chen M, Li X, Liu J, Han Y, Cheng L. Safety and pharmacodynamics of suprachoroidal injection of triamcinolone acetonide as a controlled ocular drug release model. J Control Release. 2015; 203:109–117. [PubMed: 25700623]

Chiang B, Kim YC, Doty AC, Grossniklaus HE, Schwendeman SP, Prausnitz MR. Sustained reduction of intraocular pressure by supraciliary delivery of brimonidine-loaded poly(lactic acid) microspheres for the treatment of glaucoma. J Control Release. 2016a; 228:48–57. [PubMed: 26930266]

Chiang B, Kim YC, Edelhauser HF, Prausnitz MR. Circumferential flow of particles in the suprachoroidal space is impeded by the posterior ciliary arteries. Exp Eye Res. 2016b

Culbertson C. Diffusion coefficient measurements in microfluidic devices. Talanta. 2002; 56:365–373. [PubMed: 18968508]

Einmahl S, Savoldelli M, D'Hermies F, Tabatabay C, Gurny R, Behar-Cohen F. Evaluation of a novel biomaterial in the suprachoroidal space of the rabbit eye. Invest Ophthalmol Vis Sci. 2002; 43:1533–1539. [PubMed: 11980871]

Gilger BC, Abarca EM, Salmon JH, Patel S. Treatment of acute posterior uveitis in a porcine model by injection of triamcinolone acetonide into the suprachoroidal space using microneedles. Invest Ophthalmol Vis Sci. 2013; 54:2483–2492. [PubMed: 23532526]

Goldstein DA. A phase 1/2 open-label, safety and tolerability study of triamcinolone acetonide administered to the suprachoroidal space in patients with non-infectious uveitis. Invest Ophthalmol Vis Sci. 2015; 56:3557–3557.

Gu B, Liu J, Li X, Ma Q, Shen M, Cheng L. Real-Time Monitoring of Suprachoroidal Space (SCS) Following SCS Injection Using Ultra-High Resolution Optical Coherence Tomography in Guinea Pig Eyes. Invest Ophthalmol Vis Sci. 2015; 56:3623–3634. [PubMed: 26047049]

Ianchulev, T. Suprachoroidal space as a therapeutic target. Springer; New York: 2014.

Jiang J, Gill HS, Ghate D, McCarey BE, Patel SR, Edelhauser HF, Prausnitz MR. Coated microneedles for drug delivery to the eye. Invest Ophthalmol Vis Sci. 2007; 48:4038–4043. [PubMed: 17724185]

Kadam RS, Williams J, Tyagi P, Edelhauser HF, Kompella UB. Suprachoroidal delivery in a rabbit ex vivo eye model: influence of drug properties, regional differences in delivery, and comparison with intravitreal and intracameral routes. Mol Vis. 2013; 19:1198–1210. [PubMed: 23734089]

Kim YC, Edelhauser HF, Prausnitz MR. Particle-stabilized emulsion droplets for gravity-mediated targeting in the posterior segment of the eye. Adv Healthc Mater. 2014a; 3:1272–1282. [PubMed: 24652782]

Kim YC, Edelhauser HF, Prausnitz MR. Targeted delivery of antiglaucoma drugs to the supraciliary space using microneedles. Invest Ophthalmol Vis Sci. 2014b; 55:7387–7397. [PubMed: 25212782]

Kim YC, Oh KH, Edelhauser HF, Prausnitz MR. Formulation to target delivery to the ciliary body and choroid via the suprachoroidal space of the eye using microneedles. Eur J Pharm Biopharm. 2015; 95:398–406. [PubMed: 26036448]

McDonald JH, Dunn KW. Statistical tests for measures of colocalization in biological microscopy. J Microsc. 2013; 252:295–302. [PubMed: 24117417]

Nielsen LJ, Eyley S, Thielemans W, Aylott JW. Dual fluorescent labelling of cellulose nanocrystals for pH sensing. Chem Commun (Camb). 2010; 46:8929–8931. [PubMed: 21046033]

Olsen TW, Feng X, Wabner K, Conston SR, Sierra DH, Folden DV, Smith ME, Cameron JD. Cannulation of the suprachoroidal space: a novel drug delivery methodology to the posterior segment. Am J Ophthalmol. 2006; 142:777–787. [PubMed: 16989764]

Olsen TW, Feng X, Wabner K, Csaky K, Pambuccian S, Cameron JD. Pharmacokinetics of pars plana intravitreal injections versus microcannula suprachoroidal injections of bevacizumab in a porcine model. Invest Ophthalmol Vis Sci. 2011; 52:4749–4756. [PubMed: 21447680]

Patel SR, Berezovsky DE, McCarey BE, Zarnitsyn V, Edelhauser HF, Prausnitz MR. Targeted administration into the suprachoroidal space using a microneedle for drug delivery to the posterior segment of the eye. Invest Ophthalmol Vis Sci. 2012; 53:4433–4441. [PubMed: 22669719]

Patel SR, Lin AS, Edelhauser HF, Prausnitz MR. Suprachoroidal drug delivery to the back of the eye using hollow microneedles. Pharm Res. 2011; 28:166–176. [PubMed: 20857178]

Peden MC, Min J, Meyers C, Lukowski Z, Li Q, Boye SL, Levine M, Hauswirth WW, Ratnakaram R, Dawson W, Smith WC, Sherwood MB. Ab-externo AAV-mediated gene delivery to the suprachoroidal space using a 250 micron flexible microcatheter. PLoS One. 2011; 6:e17140. [PubMed: 21347253]

Rodrigues EB, Grumann A Jr, Penha FM, Shiroma H, Rossi E, Meyer CH, Stefano V, Maia M, Magalhaes O Jr, Farah ME. Effect of needle type and injection technique on pain level and vitreal reflux in intravitreal injection. J Ocul Pharmacol Ther. 2011; 27:197–203. [PubMed: 21314588]

Tyagi P, Barros M, Stansbury JW, Kompella UB. Light-activated, in situ forming gel for sustained suprachoroidal delivery of bevacizumab. Mol Pharm. 2013; 10:2858–2867. [PubMed: 23734705]

Tzameret A, Sher I, Belkin M, Treves AJ, Meir A, Nagler A, Levkovitch-Verbin H, Barshack I, Rosner M, Rotenstreich Y. Transplantation of human bone marrow mesenchymal stem cells as a thin subretinal layer ameliorates retinal degeneration in a rat model of retinal dystrophy. Exp Eye Res. 2014; 118:135–144. [PubMed: 24239509]

Wang M, Liu W, Lu Q, Zeng H, Liu S, Yue Y, Cheng H, Liu Y, Xue M. Pharmacokinetic comparison of ketorolac after intracameral, intravitreal, and suprachoroidal administration in rabbits. Retina. 2012; 32:2158–2164. [PubMed: 23099451]

Highlights

- Studied spread in suprachoroidal space (SCS) post microneedle injection in rabbit eye
- Particles in saline were entrapped in the SCS after injection; fluorescein was not
- Particles injected with polymers co-localized while spreading in SCS for 2–4 days
- After 1–3 weeks, polymers were cleared from SCS, but particles remained in place
- Co-localization with polymer allowed spreading of particles in SCS

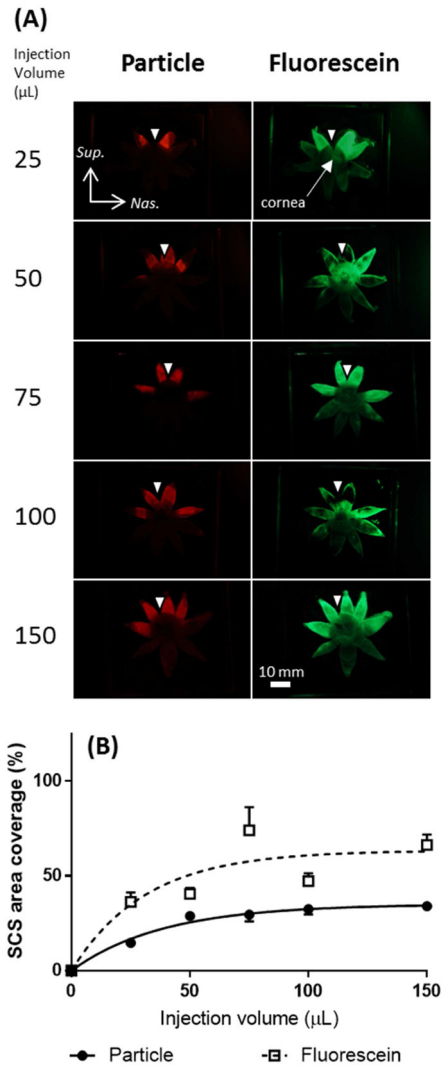

Figure 1.

Percentage area of SCS containing injected particles and fluorescein molecules, as determined by flat-mount measurement method. (A) Representative red and green fluorescence flat-mount images to visualize the spread of particles (0.2 μm diameter) and fluorescein after microneedle injection in *ex vivo* rabbit eyes. Eyes frozen and processed 3 min after injection. (B) Quantification of percent area (mean±SEM, N=3–5 replicates) of SCS covered by red particles or fluorescein. Exponential fits to the data are shown as a visual aid.

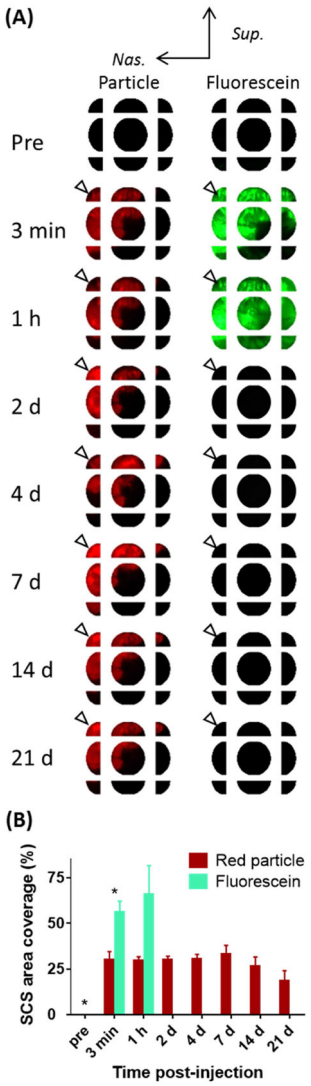

Figure 2.

Spread of particles and fluorescein molecules in the SCS after injection of HBSS formulation *in vivo*. (A) Representative fluorescent fundus collages after microneedle injection of red-fluorescent particles (0.2 μm diameter) and fluorescein in HBSS in the supranasal position *in vivo* (injection site indicated by white arrow). The same animal was imaged for the duration of the experiment. Sup.=superior. Nas.=nasal. (B) Quantification of area covered (mean±SEM, N=3) by red-fluorescent particles and fluorescein in HBSS. * represents time points where red particle and fluorescein signals co-localize.

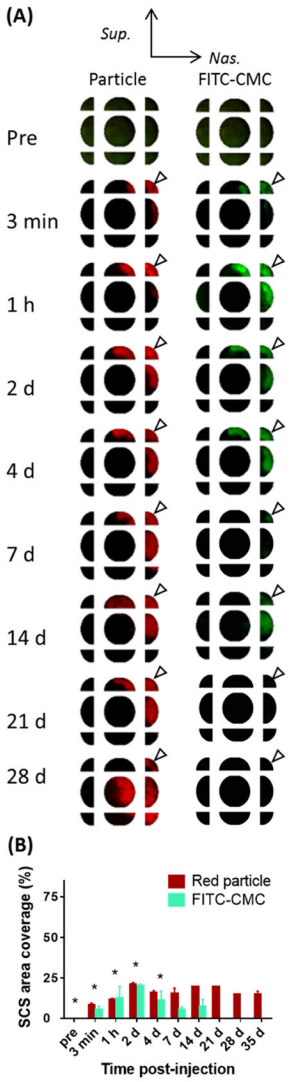

Figure 3.

Spread of particles and FITC-CMC in the SCS after injection in FITC-CMC formulation *in vivo*. (A) Representative fluorescent fundus collages after microneedle injection of red-fluorescent particles (0.2 μm diameter) and FITC-CMC in HBSS in the supranasal position (injection site indicated by white arrow). The same animal was imaged for the duration of each experiment. Sup. = superior. Nas.= nasal. (B) Quantification of area covered (mean ±SEM, N=2–4) by red fluorescent particles and FITC-CMC in HBSS. * represents time points where red particle and FITC-CMC signals co-localize.

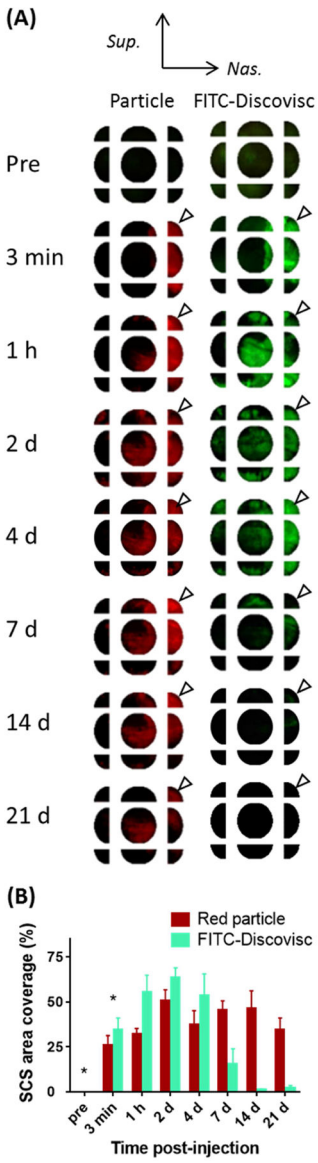

Figure 4.

Spread of particles and FITC-Discovisc in the SCS after injection in FITC-Discovisc formulation *in vivo*. (A) Representative fluorescent fundus collages after microneedle injection of red-fluorescent particles (0.2 μm diameter) and FITC-Discovisc reconstituted in HBSS in the supranasal position (injection site denoted by white arrow). The same animal was imaged for the duration of each experiment. Sup.=superior. Nas.=nasal. (C) Quantification of area covered (mean±SEM, N=2–4) by red fluorescent particles and FITC-Discovisc in HBSS. * represents time points where red particle and FITC-Discovisc signals co-localize.

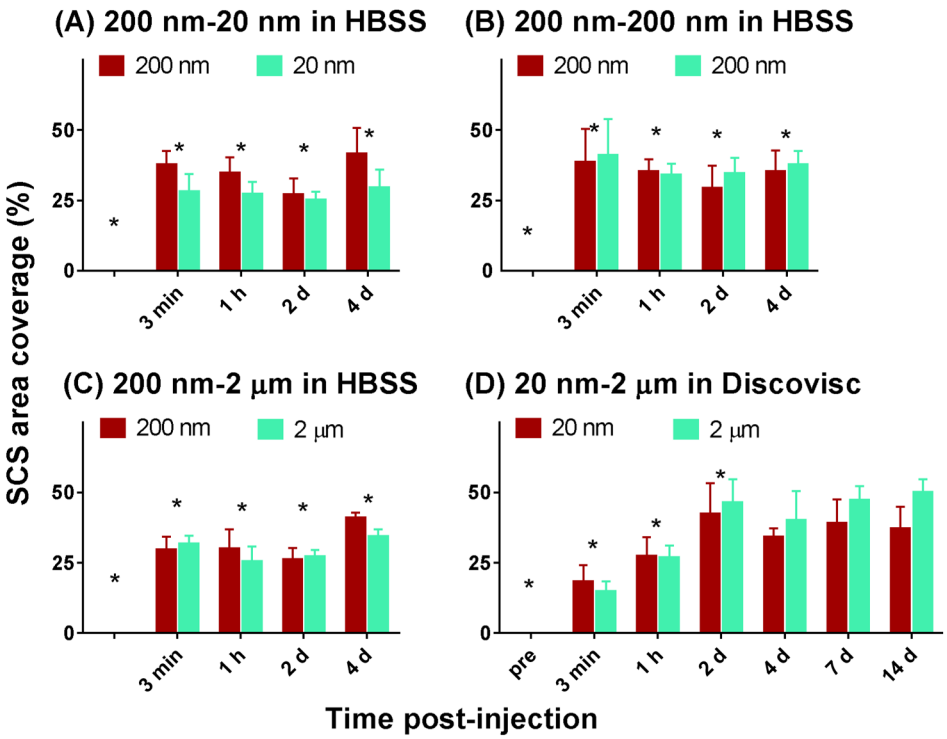

Figure 5.

Quantification of area covered (mean±SEM, N=3–4) after SCS injection with (A) 200 nm red- and 20 nm green-fluorescent particles in HBSS, (B) 200 nm red- and 200 nm green-fluorescent particles in HBSS, (C) 200 nm red- and 2 µm green-fluorescent particles in HBSS, and (D) 20 nm red- and 2 µm green-fluorescent particles in Discovisc over time *in vivo*. The same animal was imaged for the duration of each experiment. * represents time points where red- and green-fluorescent particles signals co-localize.